Journal Name

Cite this: DOI: 10.1039/c0xx00000x

www.rsc.org/xxxxxx

Supporting Information

Significant enhancement in blue emission and electrical conductivity of N-doped graphene

Tran Van Khai,[a] Han Gil Na,[a] Dong Sub Kwak,[a] Yong Jung Kwon,[a] Heon Ham,*[b] Kwang Bo Shim*[a] and Hyoun Woo Kim*[a]

[a]*Division of Materials Science and Engineering, Hanyang University, Seoul 133-791, Republic of Korea*

[b]*H&H Co. LTD, Chungju National University, 50 Daehak-ro, Chungju-si, Chungbuk, 330-702, Korea*

E-mail: hyounwoo@hanyang.ac.kr; kbshim@hanayng.ac.kr; Fax: +82-2-2220-0382

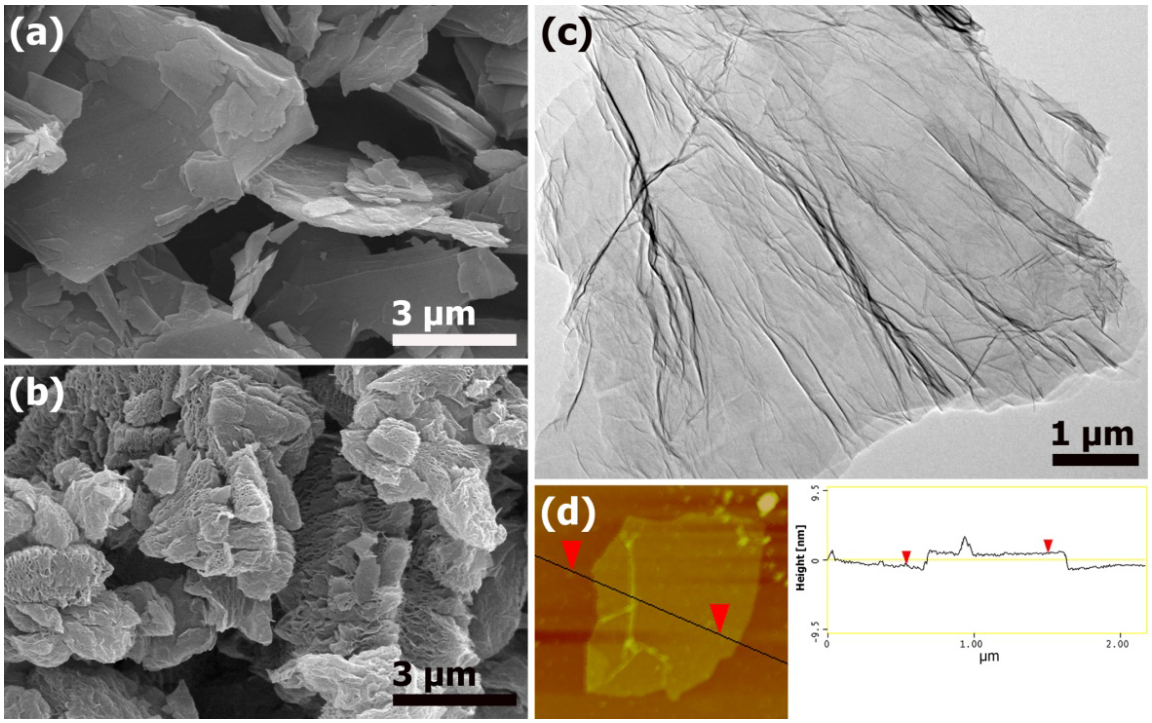

Fig. S1 SEM images of (a) graphite material,(b) air-dried RGO, (c) TEM image of RGO and (d) AFM image of RGO and the height in the selected location.

Fig. S1 shows SEM images of (a) graphite, (b) air-dried RGO, (c) TEM and (d) AFM images RGO. As can be seen in Fig. S2b, the obtained RGO material shows the layered structure. Fig. S2c shows TEM image of few layer RGO sheets. TEM images of RGO sheets generally reveal wrinkled flakes with edges that are partially folded or scrolled due to the high surface tension needed for the graphene sheets to maintain its planarity.[1,2] The thin sheets showed lateral dimensions ranging from 2 to 5 µm in size. Most RGO sheets exist in style of thin few-layer, and it was confirmed by non-contact mode AFM, as shown in Fig. S2d. The cross-sectional view of the typical AFM image of the RGO sheet indicated that the thickness of RGO sheet was in the range of 0.8-1.1 nm, corresponding to bi or tri-layer RGO sheet,[3,4] which is in agreement with the TEM result. The thickness is somewhat larger than that of monolayer pristine graphene (0.34 nm) because of the presence of residual oxygen-containing functional groups on both sides of RGO sheets.[5]

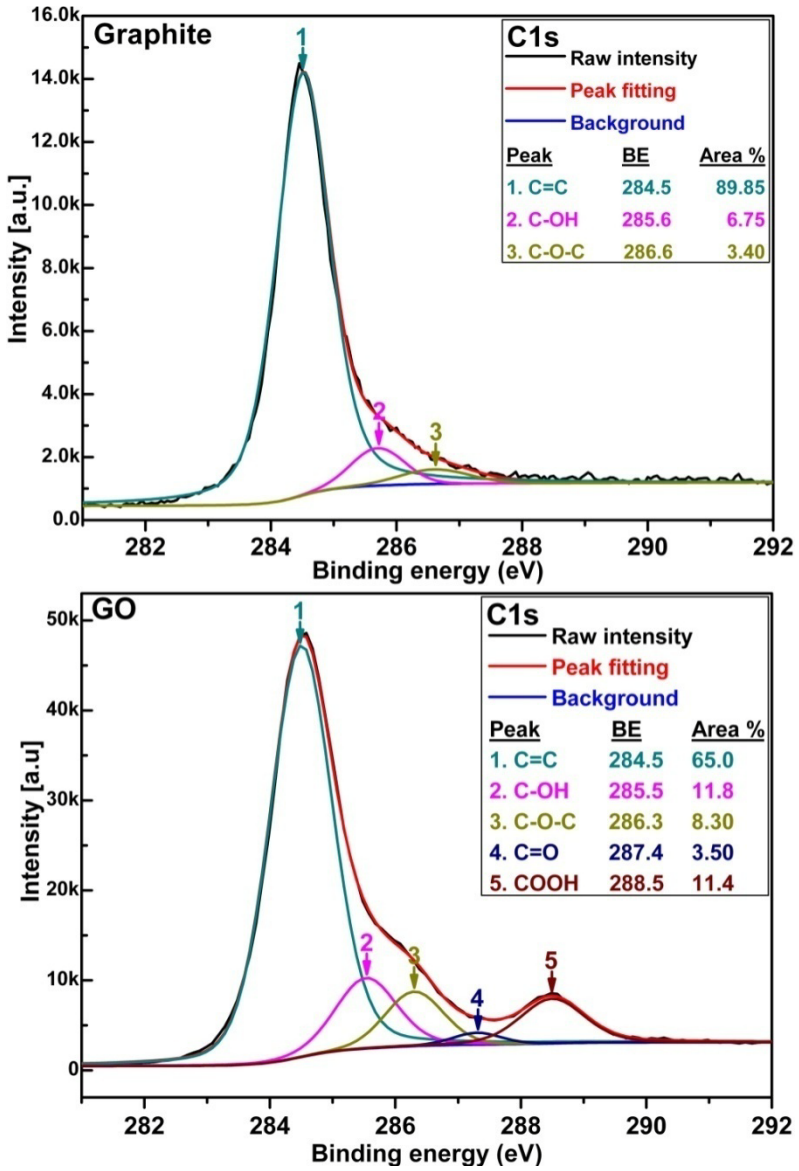

Fig. S2 High resolution C1 XPS spectra of graphite and GO

Fig. S2 shows the typical high resolution C1s XPS spectra of graphite and GO. For the graphite material, the C1s peak can be fitted to three components located at 284.5, 285.6 and 286.6 eV. The main peak at 284.5 eV corresponds to binding energy of sp^2 graphitic bonds (C=C), indicating that

most of the carbon atoms in the graphite are arranged in a conjugated honeycomb lattice (89.85% area of C=C bonds). The other peaks located at 285.6 and 286.6 eV are attributed to C-OH (hydroxyls) and C-O-C (epoxy/ether) groups, respectively. The C1s XPS spectrum of GO clearly indicates a considerable degree of oxidation with five different kinds of carbon atoms, located at 284.5, 285.5, 286.3, 287.4 and 288.5 correspondingly exist in different functional groups: C=C, C-OH, C-O-C, C=O (carbonyls), COOH (acids) groups, respectively. This indicates that the rich oxygen groups are contained within the GO.

Preparation of films on glass substrates

We prepared GO/graphene films of the same thickness on the glass substrates (1x1cm^2) from GO, RGO and N-doped RGO materials using air-brush spraying technique. The GO, RGO and N-doped RGO sheets dispersed in ethanol at the same concentration (0.1mg/mL) and sonicated for 2h. An air-brush was used to spray the as-prepared GO, RGO, and N-doped RGO suspension onto the glass substrates. The air-brush is connected to an Ar tank, and the gas pressure is adjusted by using the control vale. During film formation, the air-brush is held at a distance of 10 cm from the substrate surface and the graphene suspension stream is kept perpendicular to the substrate surface. The substrate is put on a hot-plate at about 120 ^{o}C. The thickness of film was carefully controlled by adjusting the volume of the suspension. Next, these films were dried in a vacuum oven at 90^{o}C for 24h before measuring the electrical conductivity. By using FE-SEM, thickness of these films was estimated to be about 250 nm, as shown in **Figure S3(a)**.

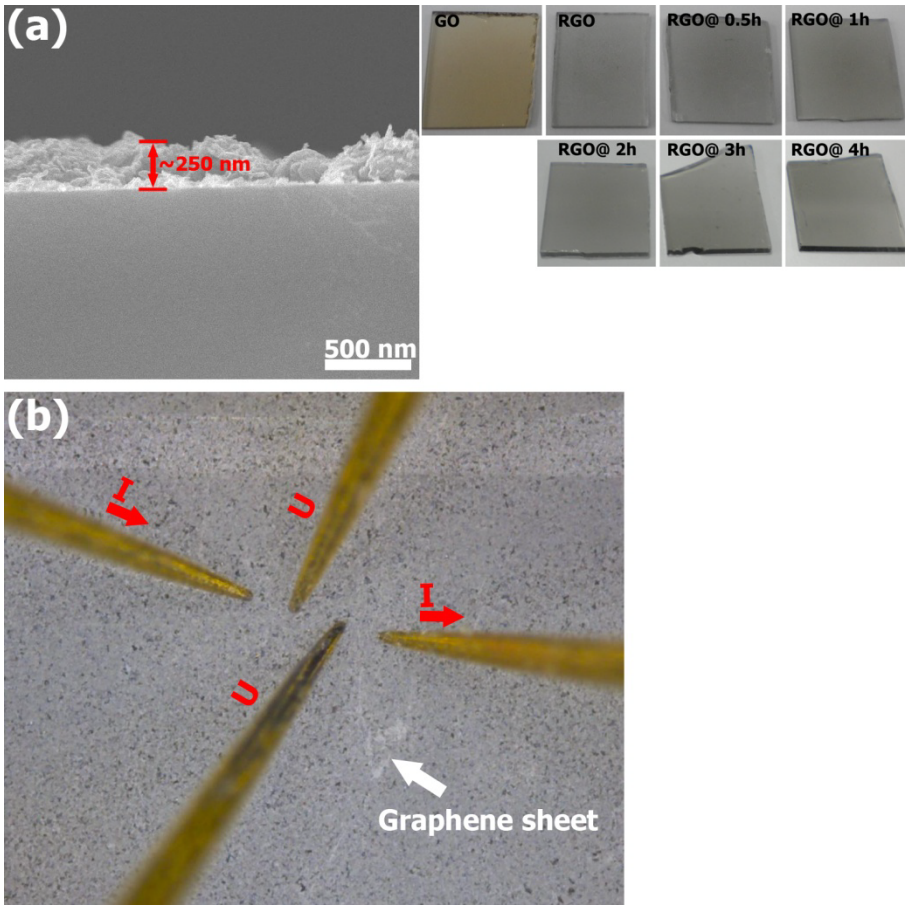

Figure 3S (a) Cross-sectional FE-SEM image of a graphene film on glass substrate, (b) optical microscopy image of the four-point probe measurement setup. The digital images of as-prepared GO, RGO, and N-doped RGO films (top right).

5

Calculating the content/ratio/area of different composition:

1. Calculating atomic concentration (at%.) of the each sample.

Table 1: Atomic sensitive factors (ASF) [6]

Element	ASF
C	0.296
O	0.711
N	0.477

Atomic concentration (at.%) is calculated by using equation (1):

$$Atomic\ \% = \frac{\frac{I_x}{S_x}}{\sum_i \frac{I_i}{S_i}} \times 100\% \qquad (1)$$

Where I_x is the relative peak area of photoelectrons from element x. S_x is atomic sensitive factor of element x (as shown in **Table 1**), $\sum_i \frac{I_i}{S_i}$ peak areas/sensitivity factors of all other elements. The peak area of the each element x is calculated from the survey scan XPS spectrum by using **XPSPEAK41** software. For example, calculating at.% of RGO@ 4h, from the survey scan SPX spectrum by using **XPSPEAK41** software, we obtain relative peak area of C, N and O:

$I_C = 12763$

$I_N = 503$

$I_O = 1884$

From the equation (1), we calculate atomic concentration:

$$C\% = \frac{\frac{12763}{0.296}}{\frac{12763}{0.296} + \frac{503}{0.477} + \frac{1844}{0.711}} \times 100\% = \frac{43118}{46765} \times 100\% = 92.20\%$$

$$N\% = \frac{\frac{503}{0.477}}{\frac{12763}{0.296} + \frac{503}{0.477} + \frac{1844}{0.711}} \times 100\% = \frac{1054}{46765} \times 100\% = 2.25\%$$

$$O\% = \frac{\frac{1884}{0.711}}{\frac{12763}{0.296} + \frac{503}{0.477} + \frac{1844}{0.711}} \times 100\% = \frac{2593}{46765} \times 100\% = 5.55\%$$

So, we have O/C (5.55/92.2 = 0.06) atomic ratio.

Similarly, we calculate atomic concentration and atomic ratio for all the samples.

2. Calculating peak area (%) of different composition of each sample.

The peak area (%) of different composition by using:

$$\text{Peak area (\%)} = \frac{A_x}{\sum_i A_i} \qquad (2)$$

Where A_x is peak area of composition x, $\sum_i A_i$ is total peak area of all other compositions. The high resolution XPS spectra were deconvoluted with a combination of Gaussian and Lorentian fitting using **XPSPEAK41** software.

For example, we calculate the peak area (%) of different composition of RGO@ 4h. For C1s peak position, by deconvoluting with a combination of Gaussian and Lorentian peaks after subtraction of background, five peaks were observed and the results were shown in **Table 2**

Table 2: C1s SPX spectrum of RGO@ 4h

Peak	Position (eV)	Area	FWHM (ev)	% Gaussian –Lorentian (%)
1	284.43	11049	1.10	40
2	285.38	978	0.72	20
3	286.00	855	1.00	20
4	289.90	379	1.23	20
5	287.80	100	0.90	25

From the peak area, we calculate peak area (%) of different compositions using equation (2):

$\mathbf{C = C}$ (284. 4 eV), peak area (%) $= \frac{11049}{11049+978+855+379+100} \times 100\% = \frac{11049}{13361} \times 100\% = \sim 82.7\%$

$\mathbf{C - OH}$ (285. 4 eV), peak area (%) $= \frac{978}{133361} \times 100\% = \sim 7.32\%$

$\mathbf{C - N\ (sp^2)}$ (286. 0 eV), peak area (%) $= \frac{855}{13361} \times 100\% = \sim 6.40\%$

$\mathbf{C - O - C}$ (286. 9 eV), peak area (%) $= \frac{379}{13361} \times 100\% = \sim 2.83\%$

$\mathbf{C - N\ (sp^3)}$ (287. 8 eV), peak area (%) $= \frac{100}{13361} \times 100\% = \sim 0.75\%$

For N1s peak position, after fitting three peaks were observed and the results were shown in Table 3

Table 3: N1s SPX spectrum of RGO@ 4h

Peak	Position (eV)	Area	FWHM (ev)	% Gaussian -Lorentian (%)
1	402.20	251	1.60	30
2	400.26	115	1.05	15
3	399.00	260	1.59	10

From the peak area, we calculate peak area (%) of different compositions:

Quanternary $-$ **N** (402. 2 eV), peak area (%) $= \frac{251}{251+115+260} \times 100\% = \frac{251}{626} \times 100\% = \sim 40.0\%$

Pyrrolic $-$ **N** (400. 2 eV), peak area (%) $= \frac{115}{626} \times 100\% = \sim 18.4\%$

Pyridine $-$ **N** (399. 0 eV), peak area (%) $= \frac{260}{626} \times 100\% = \sim 41.6\%$

Similarly, we calculate peak area (%) of different compositions for all the samples.

Reference:

1 I. Janowska, K. Chizari, O. Ersen, S. Zafeiratos, D. Soubane, V. D. Costa, V. Specisser, C. Boeglin, M. Houllé, D. Bégin, D. Plee, M. J. Ledoux and C.Pham-Huu, *Nano Res.*, 2010, **3**, 126.

2 J. C. Meyer, A. K. Geim, M. I. Katsnelson, K. S. Novoselvo, T. J. Booth and S. Roth, *Nature*, 2007, **446**, 60.

3 X. Li, H. Wang, J. T. Robinson, H. Sanchez, G. Diankov and H. Dai, *J. Am. Chem. Soc.*, 2009, **131**, 1752.

4 K. A. Mkhoyan, A. W. Contryman, J. Silcox, D. A. Stewart, G. Eda, C. Mattevi, S. Miller and M. Chhowalla, *Nano Lett.*, 2009, **9**, 1058.

5 J. I. Paredes, S. Villar-Rodil, A. Martínez-Alonso and J. M. D. Tascón, *Langmuir*, 2008, **24**, 10560.

6 J.F. Moulder et al., Handbook of X-ray Photoelectron Spectroscopy, Physical Electronics, Inc., Eden Prairie, MN, USA (1992).